

## Anomalous electronic, phonon, and spin excitations in the chalcogenide spinel FeCr<sub>2</sub>S<sub>4</sub>

K.-Y. Choi, P. Lemmens, P. Scheib, V. Gnezdilov, Yu. G. Pashkevich, Joachim Hemberger, Alois Loidl, Vladimir Tsurkan

### Angaben zur Veröffentlichung / Publication details:

Choi, K.-Y., P. Lemmens, P. Scheib, V. Gnezdilov, Yu. G. Pashkevich, Joachim Hemberger, Alois Loidl, and Vladimir Tsurkan. 2007. "Anomalous electronic, phonon, and spin excitations in the chalcogenide spinel FeCr<sub>2</sub>S<sub>4</sub>." *Journal of Physics: Condensed Matter* 19 (14): 145260. <https://doi.org/10.1088/0953-8984/19/14/145260>.

# Anomalous electronic, phonon, and spin excitations in the chalcogenide spinel $\text{FeCr}_2\text{S}_4$

K-Y Choi<sup>1</sup>, P Lemmens<sup>2,7</sup>, P Scheib<sup>2</sup>, V Gnezdilov<sup>3</sup>, Yu G Pashkevich<sup>4</sup>, J Hemberger<sup>5</sup>, A Loidl<sup>5</sup> and V Tsurkan<sup>5,6</sup>

<sup>1</sup> NHMFL/FSU, Tallahassee, FL 32310-3706, USA

<sup>2</sup> Institute for Condensed Matter Physics, TU Braunschweig, D-38106 Braunschweig, Germany

<sup>3</sup> B I Verkin Institute for Low Temp. Phys., NASU, 61164 Kharkov, Ukraine

<sup>4</sup> A A Galkin Donetsk Phystech NASU, 83114 Donetsk, Ukraine

<sup>5</sup> EP V, Center for Electronic Correlation and Magnetism, University of Augsburg, 86135 Augsburg, Germany

<sup>6</sup> Institute of Applied Physics, Acad. Sci. Moldova, MD-2028, Chisinau, Moldova

E-mail: [p.lemmens@tu-bs.de](mailto:p.lemmens@tu-bs.de)

## Abstract

We report inelastic light scattering experiments on  $\text{FeCr}_2\text{S}_4$ , which shows colossal magnetoresistance (CMR) effects around  $T_C \approx 170$  K. Several distinct features have been observed: (i) anomalies in phonon frequencies and linewidths around  $T_C$ , (ii) the vanishing of one-magnon excitation close to  $0.83 T_C$ , and (iii) the presence of an electronic background at low temperature. This highlights the significance of an intricate interplay among electron, spin, orbital, and lattice degrees of freedom in inducing CMR effects.

(Some figures in this article are in colour only in the electronic version)

## 1. Introduction

Over the last decade, a large research effort has been devoted to the investigations of colossal magnetoresistance (CMR) systems due to fascinating physical properties as well as potential for technological applications [1]. A prominent example is given in the perovskite manganites  $\text{R}_{1-x}\text{A}_x\text{MnO}_3$  (R = rare earth, A = alkaline earth) [2]. CMR is largely explained within double-exchange (DE) interaction and electron-phonon coupling. Besides, a new class of CMR systems has been found in doped magnetic semiconductors, the pyrochlore  $\text{Tl}_2\text{Mn}_2\text{O}_7$ , and the spinel  $\text{CdCr}_2\text{Se}_4$ , which do not invoke DE and Jahn-Teller (JT) distortions [3, 4]. In these systems CMR is ascribed to scattering of charge carriers by spin fluctuations.

In this situation, the chalcogenide spinel  $\text{FeCr}_2\text{S}_4$  is in a special position among the reported CMR compounds because it shares common features with magnetic semiconductors and the perovskite manganites [5–7]. From a structural point of view, it resembles  $\text{CdCr}_2\text{Se}_4$ , in

<sup>7</sup> Author to whom any correspondence should be addressed. <http://www.peter-lemmens.de>

which the DE mechanism is totally absent. However, there is evidence for significant electron–phonon coupling and correlation effects [6]. Thus, the investigation of  $\text{FeCr}_2\text{S}_4$  can bring a deeper understanding of the origin of the CMR effect observed in widely different systems.

## 2. Properties of $\text{FeCr}_2\text{S}_4$

$\text{FeCr}_2\text{S}_4$  has a cubic spinel structure where  $\text{Fe}^{2+}$  ( $3d^6$ ,  $S = 2$ ) occupies the tetrahedral A site while  $\text{Cr}^{3+}$  ( $3d^3$ ,  $S = 3/2$ ) possesses the octahedral B site [8]. The antiferromagnetic coupling of the Fe to Cr ions leads to a ferrimagnetic spin ordering,  $T_C \approx 170$  K [5]. Electronic structure calculations signal the significance of the JT activity of the  $\text{Fe}^{2+}$  ions and electronic correlation effects in explaining transport and thermodynamic properties [6]. Furthermore, several anomalies are observed in the structural and orbital sectors at low temperatures.

Among them ultrasonic measurements show a steplike change of the elastic moduli around 60 K, attributable to a structural phase transition of a first-order type [9]. In addition, transmission electron microscopy studies [10] unveil a cubic-to-triclinic symmetry reduction for temperature below 60 K, which was suggested to arise from the combined effects of tetragonal distortions of the JT active  $\text{Fe}^{2+}$  ions and a displacement of the octahedral  $\text{Cr}^{3+}$  ions. Remarkably, the orbital state at very low temperatures depends on details of the sample state [11]. Single crystals undergo a transition to an orbital glass phase whereas polycrystal samples transit to an orbital ordered state. This has been discussed in terms of geometric frustration and a dynamic-to-static JT distortion. Around  $T_C$ , lattice anomalies and the strong dependence of magnetotransport properties on hydrostatic pressure point to substantial electron–phonon and spin–lattice coupling [12–14].

In this paper, we report Raman scattering measurements of  $\text{FeCr}_2\text{S}_4$ . Raman spectroscopy can probe simultaneously excitations arising from spin, lattice, and charge degrees of freedom [15, 16] and, thus, can shed light on the microscopic origin of CMR effects. A pronounced temperature dependence of phonon frequencies and linewidths is observed around  $T_C$ , suggesting strong spin–phonon coupling. A low energy one-magnon peak fades away around  $0.83 T_C$ . This might be associated with a strong influence of electronic correlations on the spin dynamics around  $T_C$ . At very low temperature there appears an electronic background attributable to orbital fluctuations. These experimental observations all suggest a strong interplay among electron, spin, orbital, and lattice degrees of freedom, which plays an important role in inducing CMR effects.

## 3. Experimental details

Single crystals were grown using a chemical transport-reaction method from polycrystalline material obtained by a solid-state reaction [17] as described elsewhere. We used a sample from the same batch for which an extensive characterization using structural, magnetic, and transport measurements has been demonstrated [13, 14]. As-grown single crystals with shiny surfaces were used without a prior mechanical polishing. Raman scattering measurements were performed in quasi-backscattering geometry with the excitation line  $\lambda = 514.5$  nm of an  $\text{Ar}^+$  laser. The laser power of 7 mW was focused to a 0.1 mm diameter spot on the sample surface. The scattered spectra were collected on a DILOR-XY triple spectrometer and a nitrogen-cooled charge-coupled device detector.

## 4. Results and discussion

Figure 1 displays Raman spectra in  $(xx)$  and  $(xy)$  polarizations at 5 and 295 K. Here note that the small size of the studied sample does not allow for a study of all possible polarizations. To

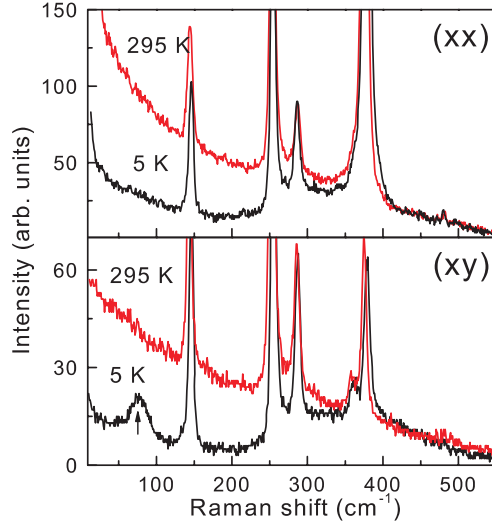


**Figure 1.** Polarization dependence of Raman spectra at 5 and 295 K in parallel ( $xx$ ) and perpendicular ( $xy$ ) polarizations, respectively. The vertical arrow indicates a peak of magnetic origin.

gain a high quality signal, light is guided to a direction whose normal surface is largest, denoted by  $x$ . Notwithstanding, it will put no significant obstacles in the way of extracting the relevant physics, since the magnetic and electronic properties of  $\text{FeCr}_2\text{S}_4$  are of 3D nature.

$\text{FeCr}_2\text{S}_4$  has the space group  $Fd\bar{3}m$ . Subtracting the acoustic modes the factor group analysis yields a total of five Raman-active modes:  $A_{1g}(aa + bb + cc) + E_g(aa + bb - 2cc, \sqrt{3}aa - \sqrt{3}bb) + 3F_{2g}(ab, bc, ca)$ . For both polarizations we observe five peaks, at 144.5, 253.6, 286, 359, and 375.6  $\text{cm}^{-1}$ , at room temperature as phonon scattering. This corresponds to what is maximally expected from the average lattice symmetry  $Fd\bar{3}m$ . With decreasing temperature no extra mode appears, although a structural transition from  $Fd\bar{3}m$  to  $F\bar{4}3m$  has been reported at low temperature [10]. This implies that deviations from the  $Fd\bar{3}m$  lattice symmetry are too subtle to be discernible using Raman spectroscopy.

Besides the lattice vibrational modes, several salient features show up: (i) a low energy magnon peak around 85  $\text{cm}^{-1}$  in ( $xy$ ) polarization, (ii) a high energy magnetic continuum with an asymmetric lineshape extending from about 240 to 500  $\text{cm}^{-1}$  in ( $xx$ ) and ( $xy$ ) polarizations, and (iii) a broad electronic background (see figures 1 and 4).

#### 4.1. Phonon modes

We will first focus on the temperature dependence of the phonon frequencies and linewidths, extracted by fitting the corresponding spectra to Lorentzian profiles. The results are summarized in figure 2.

In the paramagnetic regime, all phonon modes show a similar behaviour; upon cooling their frequencies increase nearly linearly. This is due to lattice contractions caused by lattice anharmonicities. The anomalous temperature dependence of the frequencies starts at around  $T_C$ . The internal mode of 144.5  $\text{cm}^{-1}$  undergoes a tiny hardening upon cooling below  $T_C$ . In contrast, the external modes at 253.6, 286, and 375.6  $\text{cm}^{-1}$  soften by roughly 2  $\text{cm}^{-1}$ . The observed relative frequency shifts largely amount to  $\sim 1\%$ . The onset temperature of the phonon anomalies together with their order of magnitude gives evidence for spin-phonon coupling.

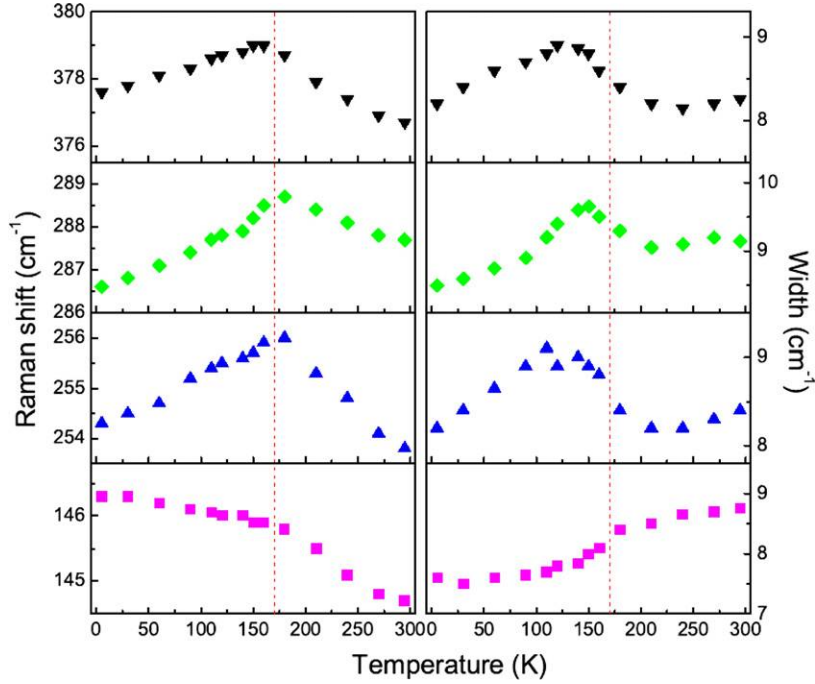


**Figure 2.** (Left panel) Temperature dependence of the peak frequencies at 144.5, 253.6, 286, and 375.6  $\text{cm}^{-1}$ . (Right panel) Phonon linewidths of the respective mode as a function of temperature.

We recall that similar phonon shifts are observed by optical spectroscopy (compare to figure 2 of [14]). On the other hand it should be mentioned that phonon anomalies in manganites are much larger in magnitude [18–20].

A remarkable observation is that all phonon modes participate in the frequency shift, irrespective of their symmetry. This implies that eigenmodes of all optic phonons are involved in superexchange paths. Actually, in  $\text{FeCr}_2\text{S}_4$  there are several exchange paths with different signs: an FM (ferromagnetic) Cr–S–Cr bond, and AFM (antiferromagnetic) Fe–S–Fe and Fe–S–Cr–S–Fe bonds. Most probably, the softening is associated with FM while the hardening should be associated with AFM. Then, the magnitude and sign of the frequency shift will be determined by the net effect of the involved exchange paths [21].

Also the linewidths exhibit an anomalous temperature dependence, which cannot be explained by anharmonic effects alone. With decreasing temperature the damping constant of the external modes increases between 140 and 200 K and then decreases monotonically. The enhanced damping in the intermediate temperature range suggests a change of the relaxation mechanism. In the respective temperature interval the resistivity exhibits anomalies [5, 6]. As a consequence, scattering of phonons by electronic excitations is expected to undergo a substantial change with the aid of electron–phonon couplings. Noticeably, ac susceptibility shows anomalies related to changes of the relaxation rate [22]. Furthermore, the one-magnon excitation disappears around the temperature where the linewidths show a peak (see below and figure 3).

#### 4.2. Magnetic excitations

Shown in figure 3(a) is the temperature dependence of the low energy excitation seen around 85  $\text{cm}^{-1}$ . With increasing temperature from 5 K it undergoes a softening and damping and then

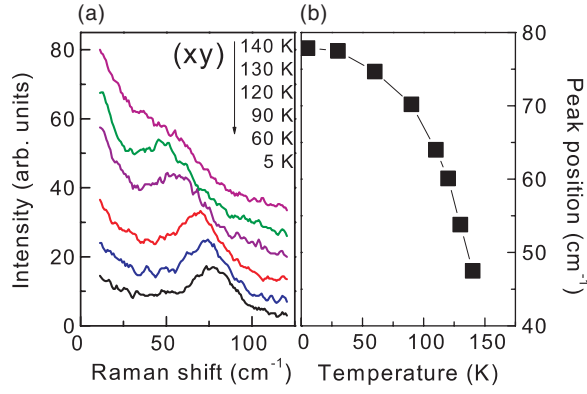


**Figure 3.** (a) Temperature dependence of magnetic Raman spectra in  $(xy)$  polarization at 5, 60, 90, 120, 130, and 140 K (from lower to upper curve). (b) Temperature dependence of the peak position.

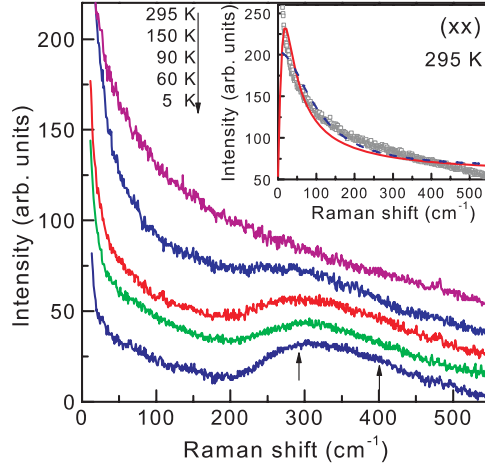


**Figure 4.** Temperature dependence of a two-magnon continuum and an electronic background at 5, 60, 90, 150, and 295 K (from lower to upper curve) in  $(xx)$  polarization. For clarity, phonon modes are subtracted by fitting them to Lorentzian profiles. Inset: the solid line represents a fitting of the diffusive scattering at 295 K to a collision-dominated model while the dashed line to a Lorentzian profile.

disappears into a diffusive background around 140 K. Furthermore, it possesses a pronounced temperature and polarization dependence: (i) it is present for temperature below  $T_C$ , (ii) the temperature dependence of the peak position shows a power-law behaviour (see figure 3(b)), and (iii) it is observed only in crossed polarization. This is characteristic for one-magnon excitations corresponding to one-spin-flip processes by virtue of non-negligible spin-orbit coupling of  $\text{Fe}^{2+}$  and  $\text{Cr}^{3+}$  ions. The notable thing is that the one-magnon signal vanishes around 140 K ( $\approx 0.83 T_C$ ), well below  $T_C$ . At first glance, this seems to be related to the gradual breakdown of a long-range magnetic order and the emergence of nanoscale magnetic clusters at much lower temperature than  $T_C$  as Mössbauer spectroscopy measurements [23] have reported. However, our samples do not show any indication for the formation of such clusters [24]. We recall that the vanishing of the one-magnon signal takes place at the temperature where the

resistivity exhibits a steplike drop [5, 6]. Thus, a change of electronic correlations might be responsible for this.

Figure 4 displays the temperature dependence of the broad magnetic signal and electronic background in  $(xx)$  polarization. For clarity, the five phonon peaks are subtracted after fitting them to Lorentzian profiles. The resulting spectra show a substantial temperature-induced rearrangement of spectral weight. At 5 K the asymmetric, broad continuum extending from about 240 to 500  $\text{cm}^{-1}$  is observed together with the electronic background below about 200  $\text{cm}^{-1}$ . With increasing temperature the continuum becomes damped and renormalized and finally merges into the diffusive background at high temperatures. This is typical for two-magnon (2M) Raman scattering arising from a double spin-flip process of a ferrimagnetic ground state ( $S = 2, S_z = 2$  and  $S = 3/2, S_z = -3/2$ ) to a higher state ( $S = 2, S_z = 1$  and  $S = 3/2, S_z = -1/2$ ). In the classical limit, the peak position of 2M scattering is given by  $J(2zS - 1)$ , where  $J$  is the exchange constant,  $z$  is the number of nearest neighbouring spins, and  $S$  is the spin number [25]. For a ferrimagnetic ground state with a spinel structure there are two characteristic peak energies given by 17 and 25 J. We have analysed the broad spectrum at 5 K in terms of two Gaussian profiles by approximating the electronic background as a Lorentzian profile (not shown here). We are able to identify two peaks at 278 and 369  $\text{cm}^{-1}$ . They yield  $J = 16.4$  and 14.8  $\text{cm}^{-1}$ , respectively. In spite of the simple estimate, the agreement is reasonable. From this, one obtains the unrenormalized AF exchange constant of  $J = 21.2\text{--}23.5$  K between Fe and Cr ions.

#### 4.3. Electronic scattering

We will turn now to the electronic background observed below  $\sim 200 \text{ cm}^{-1}$  at 5 K. With increasing temperature, it merges into quasielastic scattering arising from the overdamped 2M continuum. In semiconductors an electronic Raman response arises from impurities, short-range charge, and spin fluctuations. For temperature much below  $T_C$ , spin fluctuations will not give a dominant contribution. It is worth noting that heat-capacity measurements [11] show a transition from an orbital liquid to an orbital glass state around 10 K. Therefore, the electronic response might be due to scattering from orbital fluctuations. Also, the manganites exhibit pronounced electronic response of the same origin, which is described in terms of the collision-dominated (CD) model with the scattering rate of  $10^2\text{--}10^3$ , depending on the bandwidth [26]. However, in our case there exist substantial deviations from the CD model in the overall temperature range (not shown here). While this is partly caused by an ambiguity in determining the full spectral weight due to the overlap with the magnetic continuum, it may also reflect the presence of other excitations. Besides the strong AF interaction, there is weak FM interaction between Cr ions and AFM interaction between Fe ions. They might give weak contributions for frequencies below  $\sim 200 \text{ cm}^{-1}$ . The temperature dependence of the electronic response is complicated due to an enhanced scattering from spin fluctuations as well as due to quasielastic response arising from pure spin correlations. This is reflected in deviations of the diffusive scattering at 295 K from both the CD model and a Lorentzian profile (see the inset of figure 4). This might signify a more important role of spin-disorder scattering in  $\text{FeCr}_2\text{S}_4$  than in the manganites. Thus, we conclude that spin fluctuations should also be considered in explaining the CMR effect.

## 5. Conclusions

In summary, we have presented Raman scattering measurements of the chalcogenide spinel  $\text{FeCr}_2\text{S}_4$ . We observe phonon anomalies around  $T_C$ , the disappearance of a one-magnon

peak for temperature well below  $T_C$ , and the presence of an electronic background at low temperatures. This evidences an intricate interplay among electron, spin, orbital, and lattice degrees of freedom, suggesting a strongly correlated nature of the studied compound. Therefore, our study suggests that the CMR of  $\text{FeCr}_2\text{S}_4$  is driven by the combined effects of spin fluctuations and electron–phonon coupling.

## Acknowledgments

This work was supported by DFG and ESF-HFM.

## References

- [1] Tokura Y (ed) 2000 *Colossal Magnetoresistive Oxides* (London: Gordon and Breach)
- [2] Tokura Y and Nagaosa N 2000 *Science* **288** 462
- [3] Subramanian M A, Toby B H, Ramirez A P, Marshall W J, Sleight A W and Kwei G H 1996 *Science* **273** 81
- [4] Majumdar P and Littlewood P B 1998 *Nature* **395** 479
- [5] Ramirez A P, Cava R J and Krajewski J 1997 *Nature* **386** 156
- [6] Park M S, Kwon S K, Youn S J and Min B I 1999 *Phys. Rev. B* **59** 10018
- [7] Johansson M and Lemmens P 2006 *Crystallography and Chemistry of Perovskites (Handbook of Magnetism and Advanced Magnetic Media)* ed H Kronmüller (New York: Wiley) (Preprint cond-mat/0506606)
- [8] Haacke G and Beegle L C 1967 *J. Phys. Chem. Solids* **28** 1699
- [9] Maurer D, Tsurkan V, Horn S and Tidecks R 2003 *J. Appl. Phys.* **93** 9173
- [10] Mertinat M, Tsurkan V, Samusi D, Tidecks R and Haider F 2005 *Phys. Rev. B* **71** 100408(R)
- [11] Fichtl R, Tsurkan V, Lunkenheimer P, Hemberger J, Fritsch V, Krug von Nidda H-A, Scheidt E-W and Loidl A 2005 *Phys. Rev. Lett.* **94** 027601
- [12] Tachibana M, Akiyama K, Yoshizawa M, Kawaji H and Atake T 2005 *Phys. Rev. B* **71** 180403(R)
- [13] Fritsch V, Deisenhofer J, Fichtl R, Hemberger J, Krug von Nidda H-A, Mücksch M, Nicklas M, Samusi D, Thompson J D, Tidecks R, Tsurkan V and Loidl A 2003 *Phys. Rev. B* **67** 144419
- [14] Rudolf T, Pucher K, Mayer F, Samusi D, Tsurkan V, Tidecks R, Deisenhofer J and Loidl A 2005 *Phys. Rev. B* **72** 014450
- [15] Lemmens P and Choi K Y 2005 *Scattering: Inelastic Scattering Technique—Raman (Encyclopaedia of Condensed Matter Physics)* ed G Bassani, G Liedl and P Wyder (Amsterdam: Elsevier)
- [16] Lemmens P, Choi K Y, Caimi G, Degiorgi L, Kovaleva N N, Seidel A and Chou F C 2004 *Phys. Rev. B* **70** 134429
- [17] Kurmaev E Z, Postnikov A V, Palmer H M, Greaves C, Bartkowski St, Tsurkan V, Demeter M, Hartmann D, Neumann M, Zatssepina D A, Galakhov V R, Shamin S N and Trofimova V 2000 *J. Phys.: Condens. Matter* **12** 5411
- [18] Choi K Y, Lemmens P, Güntherodt G, Pashkevich Yu G, Gnezdilov V P, Reutler P, Pinsard-Gaudart L, Büchner B and Revcolevschi A 2005 *Phys. Rev. B* **71** 174402
- [19] Choi K Y, Lemmens P, Güntherodt G, Pashkevich Yu G, Gnezdilov V P, Reutler P, Pinsard-Gaudart L, Büchner B and Revcolevschi A 2005 *Phys. Rev. B* **72** 024301
- [20] Choi K-Y, Pashkevich Yu G, Gnezdilov V P, Güntherodt G, Yeremenko A V, Nabok D A, Kamenev V I, Barilo S N, Shiryaev S V, Soldatov A G and Lemmens P 2006 *Phys. Rev. B* **74** 064406
- [21] Baltensperger W 1970 *J. Appl. Phys.* **41** 1052
- [22] Tsurkan V, Hemberger J, Klemm M, Klimm S, Loidl A, Horn S and Tidecks R 2001 *J. Appl. Phys.* **90** 4639
- [23] Nath A, Klencsár Z, Kuzmann E, Homonnay Z, Vértés A, Simopoulos A, Devlin E, Kallias G, Ramirez A P and Cava R J 2002 *Phys. Rev. B* **66** 212401
- [24] Tsurkan V, Lohmann M, Krug von Nidda H-A, Loidl A, Horn S and Tidecks R 2001 *Phys. Rev. B* **63** 125209
- [25] Cottam M G and Lockwood D J 1986 *Light Scattering in Magnetic Solids* (New York: Wiley)
- [26] Choi K-Y, Lemmens P, Güntherodt G, Pattabiraman M, Rangarajan G, Gnezdilov V P, Balakrishnan G, McK Paul D and Rees M R 2003 *J. Phys.: Condens. Matter* **15** 3333